of autosomal recessive diseases that manifest in the offspring of consanguineous relationships.

In conclusion, we rapidly identified a nonsense mutation in *MCT8* in a family with X-linked leucoencephalopathy using only a single lane of exome sequencing. This method is powerful for unbiased screening of disease-related mutations in X-linked or recessive conditions.

Acknowledgements We thank the family for their participation in this study.

Funding This work was supported by research grants from the Ministry of Health, Labour and Welfare (to HO, HSa, NMa and NMi), a grant-in-aid for scientific research from the Japan Society for the Promotion of Science (NMa), a grant-in-aid for young scientists from the Japan Society for the Promotion of Science (HSa), a grant from the 2010 Strategic Research Promotion of Yokohama City University (NMa), research grants from the Japan Epilepsy Research Foundation (HSa) and a research grant from the Naito Foundation (NMa). The study sponsors had no role in the study design; in the collection, analysis, and interpretation of the data; in the writing of the report; or in the decision to submit the paper for publication.

Competing interests None.

Patient consent Obtained.

Ethics approval This study was conducted with the approval of the institutional review board of Kanagawa Children's Medical Center and Yokohama City University School of Medicine.

Provenance and peer review Not commissioned; externally peer reviewed.

REFERENCES

1. **Shendure J,** Ji H. Next-generation DNA sequencing. *Nat Biotechnol* 2008;**26**:1135–45.
2. **Wheeler DA,** Srinivasan M, Egholm M, Shen Y, Chen L, McGuire A, He W, Chen YJ, Makhijani V, Roth GT, Gomes X, Tartaro K, Niazi F, Turcotte CL, Irzyk GP, Lupski JR, Chinault C, Song XZ, Liu Y, Yuan Y, Nazareth L, Qin X, Muzny DM, Margulies M, Weinstock GM, Gibbs RA, Rothberg JM. The complete genome of an individual by massively parallel DNA sequencing. *Nature* 2008;**452**:872–6.
3. **Ng SB,** Turner EH, Robertson PD, Flygare SD, Bigham AW, Lee C, Shaffer T, Wong M, Bhattacharjee A, Eichler EE, Bamshad M, Nickerson DA, Shendure J. Targeted capture and massively parallel sequencing of 12 human exomes. *Nature* 2009;**461**:272–6.
4. **Choi M,** Scholl UI, Ji W, Liu T, Tikhonova IR, Zumbo P, Nayir A, Bakkaloglu A, Ozen S, Sanjad S, Nelson-Williams C, Farhi A, Mane S, Lifton RP. Genetic diagnosis by whole exome capture and massively parallel DNA sequencing. *Proc Natl Acad Sci U S A* 2009;**106**:19096–101.
5. **Hodges E,** Xuan Z, Balija V, Kramer M, Molla MN, Smith SW, Middle CM, Rodesch MJ, Albert TJ, Hannon GJ, McCombie WR. Genome-wide in situ exon capture for selective resequencing. *Nat Genet* 2007;**39**:1522–7.
6. **Ng SB,** Buckingham KJ, Lee C, Bigham AW, Tabor HK, Dent KM, Huff CD, Shannon PT, Jabs EW, Nickerson DA, Shendure J, Bamshad MJ. Exome sequencing identifies the cause of a mendelian disorder. *Nat Genet* 2010;**42**:30–5.
7. **Nannya Y,** Sanada M, Nakazaki K, Hosoya N, Wang L, Hangaishi A, Kurokawa M, Chiba S, Bailey DK, Kennedy GC, Ogawa S. A robust algorithm for copy number detection using high-density oligonucleotide single nucleotide polymorphism genotyping arrays. *Cancer Res* 2005;**65**:6071–9.
8. **Li H,** Ruan J, Durbin R. Mapping short DNA sequencing reads and calling variants using mapping quality scores. *Genome Res* 2008;**18**:1851–8.
9. **Dumitrescu AM,** Liao XH, Best TB, Brockmann K, Refetoff S. A novel syndrome combining thyroid and neurological abnormalities is associated with mutations in a monocarboxylate transporter gene. *Am J Hum Genet* 2004;**74**:168–75.
10. **Friesema EC,** Grueters A, Biebermann H, Krude H, von Moers A, Reeser M, Barrett TG, Mancilla EE, Svensson J, Kester MH, Kuiper GG, Balkassmi S, Uitterlinden AG, Koehrle J, Rodien P, Halestrap AP, Visser TJ. Association between mutations in a thyroid hormone transporter and severe X-linked psychomotor retardation. *Lancet* 2004;**364**:1435–7.
11. **Frints SG,** Lenzner S, Bauters M, Jensen LR, Van Esch H, des Portes V, Moog U, Macville MV, van Roozendaal K, Schrander-Stumpel CT, Tzschach A, Marynen P, Fryns JP, Hamel B, van Bokhoven H, Chelly J, Beldjord C, Turner G, Gecz J, Moraine C, Raynaud M, Ropers HH, Froyen G, Kuss AW. *MCT8* mutation analysis and identification of the first female with Allan-Herndon-Dudley syndrome due to loss of *MCT8* expression. *Eur J Hum Genet* 2008;**16**:1029–37.
12. **Vaurs-Barriere C,** Deville M, Sarret C, Giraud G, Des Portes V, Prats-Vinas JM, De Michele G, Dan B, Brady AF, Boespflug-Tanguy O, Touraine R. Pelizaeus-Merzbacher-Like disease presentation of *MCT8* mutated male subjects. *Ann Neurol* 2009;**65**:114–18.
13. **Bianco AC,** Salvatore D, Gereben B, Berry MJ, Larsen PR. Biochemistry, cellular and molecular biology, and physiological roles of the iodothyronine selenodeiodinases. *Endocr Rev* 2002;**23**:38–89.
14. **Friesema EC,** Ganguly S, Abdalla A, Manning Fox J, Halestrap AP, Visser TJ. Identification of monocarboxylate transporter 8 as a specific thyroid hormone transporter. *J Biol Chem* 2003;**41**:40128–35.
15. **Lafreniere RG,** Carrel L, Willard HF. A novel transmembrane transporter encoded by the XPCT gene in Xq13.2. *Hum Mol Genet* 1994;**3**:1133–9.
16. **Dumitrescu AM,** Liao XH, Weiss RE, Millen K, Refetoff S. Tissue-specific thyroid hormone deprivation and excess in monocarboxylate transporter (mct) 8-deficient mice. *Endocrinology* 2006;**147**:4036–43.
17. **Maranduba CM,** Friesema EC, Kok F, Kester MH, Jansen J, Sertie AL, Passos-Bueno MR, Visser TJ. Decreased cellular uptake and metabolism in Allan-Herndon-Dudley syndrome (AHDS) due to a novel mutation in the MCT8 thyroid hormone transporter. *J Med Genet* 2006;**43**:457–60.
18. **Namba N,** Etani Y, Kitaoka T, Nakamoto Y, Nakacho M, Bessho K, Miyoshi Y, Mushiake S, Mohri I, Arai H, Taniike M, Ozono K. Clinical phenotype and endocrinological investigations in a patient with a mutation in the MCT8 thyroid hormone transporter. *Eur J Pediatr* 2008;**167**:785–91.
19. **Herzovich V,** Vaiani E, Marino R, Dratler G, Lazzati JM, Tilitzky S, Ramirez P, Iorcansky S, Rivarola MA, Belgorosky A. Unexpected peripheral markers of thyroid function in a patient with a novel mutation of the MCT8 thyroid hormone transporter gene. *Horm Res* 2007;**67**:1–6.

Human Mutation
OFFICIAL JOURNAL
HGVS
HUMAN GENOME VARIATION SOCIETY
www.hgvs.org

A Response to: Loss of Dermatan-4-sulfotransferase 1 (D4ST1/CHST14) Function Represents the First Dermatan Sulfate Biosynthesis Defect, "Dermatan Sulfate-Deficient Adducted Thumb–Clubfoot Syndrome". Which Name is Appropriate, "Adducted Thumb–Clubfoot Syndrome" or "Ehlers–Danlos Syndrome"?

We thank Janecke et al. [2011] for their letter about a recently recognized dermatan 4-O-sulfotransferase 1 (D4ST1) deficiency caused by loss-of-function *CHST14* (MIM# 608429) mutations, independently found in an arthrogryposis syndrome "Adducted Thumb–Clubfoot Syndrome" (ATCS) [Dündar et al., 2009], a specific form of Ehlers-Danlos syndrome (EDS) as we have proposed (EDS, Kosho Type; EDSKT) [Miyake et al., 2010], and a subset of kyphoscoliosis type EDS without evidence of lysyl hydroxylase deficiency (EDS type VIB) coined as "Musculocontractural EDS" (MCEDS) [Malfait et al., 2010]. Janecke et al. [2011] proposed that these three conditions constitute a clinically recognizable and genetically identical type of connective tissue disorder and that the disorders should not be categorized into a form of EDS, but be termed collectively "Dermatan Sulfate-Deficient Adducted Thumb–Clubfoot Syndrome" to avoid possible confusion for both clinicians and researchers. The proposal is based on their clinical and molecular recognition of the disorder. First, the presence of multiple congenital malformations such as facial dysmorphism, cleft lip/palate, intestinal abnormalities, renal abnormalities, and features such as nephrolithiasis and muscle hypotonia in these patients are not typical in EDS, though features such as joint laxity, skin hyperextensibility/fragility, and bleeding diathesis are typical in EDS. Second, the molecular basis in the disorder is different from that in EDS.

EDS comprises a heterogeneous group of heritable connective tissue disorders, with the hallmarks being skin hyperextensibility, joint hypermobility, and tissue fragility affecting the skin, ligaments, joints, blood vessels, and internal organs [Steinmann et al., 2002]. Dominant-negative effects or haploinsufficiency of mutant procollagen α-chain genes or deficiency of collagen-processing enzymes have been found to cause EDS [Mao and Bristow, 2001]. In a revised nosology, EDS was classified into six major types [Beighton et al., 1998] and several other forms have also been identified based on the molecular and biochemical abnormalities [Abu et al., 2008; Giunta et al., 2008; Kresse et al., 1987; Schalkwijk et al., 2001; Schwarze et al., 2004].

Homozygous or compound heterozygous *CHST14* mutations have been found in 11 patients aged 0 day to 6 years at the initial publication (from four families) with ATCS [Dündar et al., 1997, 2001, 2009; Janecke et al., 2001; Sonoda and Kouno, 2000], in six patients aged 2–32 years (from six families) with EDSKT [Kosho et al., 2005, 2010; Miyake et al., 2010; Yasui et al., 2003], and in three patients aged 12–22 years (from two families) with MCEDS [Malfait et al., 2010]. Lack of detailed clinical information from later childhood to adulthood in ATCS and lack of detailed clinical information from birth to early childhood in EDSKT and MCEDS have made it difficult to determine whether the three conditions would be distinct clinical entities or a single clinical entity with variable expressions and with different presentations depending on the patients' ages at diagnosis [Miyake et al., 2010], though the latter notion was suspected to be appropriate [Janecke et al., 2011; Malfait et al., 2010]. We, therefore, have just published an article in *American Journal of Medical Genetics Part A*, describing detailed clinical findings and courses of two additional unrelated EDSKT patients, aged 2 and 6 years, which could definitely unite the three conditions [Shimizu et al., 2011]. Furthermore, we have presented a comprehensive review of all reported patients with D4ST1 deficiency, which concludes that the three conditions constitute a clinically recognizable disorder, characterized by progressive multisystem fragility-related manifestations and various malformations and allows us to term the disorder "D4ST1-deficient EDS" [Shimizu et al., 2011]. The clinical manifestations are summarized in Table 1.

We have categorized D4ST1 deficiency into a form of EDS for substantial reasons. Clinically, the disorder satisfies all the hallmarks of EDS [Steinmann et al., 2002]. All patients we have encountered were diagnosed with EDS and have been managed as having generalized connective tissue fragility, such as preventing skin wounds, hematomas, joint dislocations, and progressive talipes and spinal deformities. Careful surgical suturing of torn skin and regular evaluations of internal organs (e.g., cardiac valve abnormalities, aortic root dilation, and bladder enlargement) and ocular abnormalities are also conducted. ATCS is surely a helpful term to detect and diagnose patients at birth, but it is indeed questionable whether the term would be appropriate for the lifelong management of patients with the disorder. Furthermore, clinical manifestations extending beyond the core features of EDS are considered not as excluding information from EDS as Janecke et al. [2011] have claimed, but as wide clinical variability in EDS such as muscle hypotonia and chronic pain in most of the types, talipes equinovarus and facial characteristics in vascular type, and congenital hip dislocation in arthrochalasia type [Beighton et al., 1998; Voermans et al., 2009].

Etiologically, multisystem fragility in D4ST1 deficiency was illustrated to be caused by impaired assembly of collagen fibrils resulting from loss of dermatan sulfate (DS) in the decorin glycosaminoglycan side chain [Miyake et al., 2010], which justifies terming the

This article was published online on 24 August 2011 as DOI.10.1002/humu.21594. In order to rectify a technical error, it has been republished on 30 September 2011 as DOI.10.1002/humu.21586.

Table 1. Clinical Manifestations in D4ST1 Deficiency

Craniofacial	*Cardiovascular*
Large fontanelle (early childhood)	Congenital heart defects (ASD)
Hypertelorism	Valve abnormalities (MVP, MR, AR, ARD)
Short and downslanting palpebral fissures	Large subcutaneous hematomas
Blue sclerae	*Gastrointestinal*
Short nose with hypoplastic columella	Constipation
Ear deformities (prominent, posteriorly rotated, low set)	Diverticula perforation
Palatal abnormalities (high, cleft)	*Respiratory*
Long philtrum and thin upper lip	(Hemo) pneumothorax
Small mouth/microretrognathia (infancy)	*Urogenital*
Slender face with protruding jaw (from school age)	Nephrolithiasis/cystolithiasis
Asymmetric face (from school age)	Hydronephrosis
Skeletal	Dilated/atonic bladder
Marfanoid habitus/slender build	Inguinal hernia
Congenital multiple contractures (fingers, wrists, hips, feet)	Cryptorchidism
Recurrent/chronic joint dislocations	Poor breast development
Pectus deformities (flat, excavated)	*Ocular*
Spinal deformities (scoliosis, kyphoscoliosis)	Strabismus
Peculiar fingers (tapering, slender, cylindrical)	Refractive errors (myopia, astigmatism)
Progressive talipes deformilies (valgus, planus, cavum)	Glaucoma/elevated intraocular pressure
Cutaneous	Microcornea/microphthalmia
Hyperextensibility/redundancy	Retinal detachment
Bruisability	*Hearing*
Fragility/atrophic scars	Hearing impairment
Fine/acrogeria-like palmar creases	*Neurological*
Hyperalgesia to pressure	Ventricular enlargement/asymmetry
Recurrent subcutaneous infections/fistula	*Development*
	Hypotonia/gross motor delay

ASD: atrial septal defect; MVP: mitral valve prolapse; MR: mitral valve regurgitation; AR: aortic valve regurgitation; ARD: aortic rot dilation.

disorder a form of EDS. However, ultrastructural findings in the skin from patients with ATCS and MCEDS were not consistent with those in patients with EDSKT, characterized by intact collagen fibrils not assembled regularly or tightly [Miyake et al., 2010]. For patients with ATCS, the skin was assessed as normal [Dündar et al., 2009]. For those with MCEDS, most collagen bundles were found to be small sized, some of which were composed of variable diameter collagen fibrils separated by irregular interfibrillar spaces [Malfait et al., 2010]. Ultrastructural and glycobiological studies on the skin from other patients as well as those on other affected tissues such as bone, muscle, and intestine would be necessary to delineate the wide spectrum of pathophysiology. Involvement of other DS-containing proteoglycans such as biglycan should also be investigated. Various malformations observed in the disorder might not simply be explained by connective tissue fragility, as they are considered to be inborn errors of development [Dündar et al., 2009; Zhang et al., 2010].

Based on the clinical, molecular, ultrastructural, and glycobiological data to date, D4ST1 deficiency is characterized by a unique set of clinical features consisting of progressive multisystem fragility-related manifestations and various malformations (Table 1). Further clinical and etiological evidences would solve the problem regarding which name should be the most appropriate: "Dermatan Sulfate-Deficient Adducted Thumb-Clubfoot Syndrome" or "D4ST1-Deficient EDS." Until then, we propose that the name "D4ST1-Deficient EDS (Adducted Thumb-Clubfoot Syndrome)" would be preferable.

References

Abu A, Frydman M, Marek D, Pras E, Nir U, Reznik-Wolf H, Pras E. 2008. Deleterious mutations in the zinc-finger 469 gene cause brittle cornea syndrome. Am J Hum Genet 82:1217–1222.

Beighton P, De Paepe A, Steinmann B, Tsipouras P, Wenstrup R. 1998. Ehlers–Danlos syndromes: revised nosology, Villefranche, 1997. Am J Med Genet 77:31–37.

Dündar M, Demiryilmaz F, Demiryilmaz I, Kumandas S, Erkilic K, Kendirch M, Tuncel M, Ozyazgan I, Tolmie JL. 1997. An autosomal recessive adducted thumb-club foot syndrome observed in Turkish cousins. Clin Genet 51:61–64.

Dündar M, Kurtoglu S, Elmas B, Demiryilmaz F, Candemir Z, Ozkul Y, Durak AC. 2001. A case with adducted thumb and club foot syndrome. Clin Dysmorphol 10:291–293.

Dündar M, Müller T, Zhang Q, Pan J, Steinmann B, Vodopiutz J, Gruber R, Sonoda T, Krabichler B, Utermann G, Baenziger JU, Zhang L, Janecke AR. 2009. Loss of dermatan-4-sulfotransferase 1 function results in adducted thumb-clubfoot syndrome. Am J Hum Genet 85:873–882.

Giunta C, Elçioglu NH, Albrecht B, Eich G, Chambaz C, Janecke A, Yeowell H, Weis MA, Eyre DR, Kraenzlin M, Steinmann B. 2008. Spondylocheiro dysplastic form of the Ehlers-Danlos syndrome-an autosomal recessive entity caused by mutations in the zinc transporter gene *SLC*39A13. Am J Hum Genet 82:1290–1305.

Janecke AR, Baenziger JU, Müller T, Dündar M. 2011. Letter to the Editors. Loss of dermatan-4-sulfotransferase 1 (D4ST1/*CHST14*) function represents the first dermatan sulfate biosynthesis defect, "Dermatan sulfate-deficient adducted thumb-clubfoot syndrome". Hum Mutat 32:484–485.

Janecke AR, Unsinn K, Kreczy A, Baldissera I, Gassner I, Neu N, Utermann G, Müller T. 2001. Adducted thumb-club foot syndrome in sibs of a consanguineous Austrian family. J Med Genet 38:265–269.

Kosho T, Miyake N, Hatamochi A, Takahashi J, Kato H, Miyahara T, Igawa Y, Yasui H, Ishida T, Ono K, Kosuda T, Inoue A, Kohyama M, Hattori T, Ohashi H, Nishimura G, Kawamura R, Wakui K, Fukushima Y, Matsumoto N. 2010. A new Ehlers–Danlos syndrome with craniofacial characteristics, multiple congenital contractures, progressive joint and skin laxity, and multisystem fragility-related manifestations. Am J Med Genet Part A 152A:1333–1346.

Kosho T, Takahashi J, Ohashi H, Nishimura G, Kato H, Fukushima Y. 2005. Ehlers–Danlos syndrome type VIB with characteristic facies, decreased curvatures of the spinal column, and joint contractures in two unrelated girls. Am J Med Genet Part A 138A:282–287.

Kresse H, Rosthoj S, Quentin E, Hollmann J, Glossl J, Okada S, Tonnesen T. 1987. Glycosaminoglycan-free small proteoglycan core protein is secreted by fibroblasts from a patient with a syndrome resembling progeroid. Am J Hum Genet 41:436–453.

Malfait F, Syx D, Vlummens P, Symoens S, Nampoothiri S, Hermanns-Lê, Van Lear L, De Paepe A. Musculocontractural Ehlers–Danlos syndrome (former EDS type VIB) and adducted thumb clubfoot syndrome (ATCS) represent a single clinical entity caused by mutations in the dermatan-4-sulfotransferase 1 encoding *CHST14* gene. 2010. Hum Mutat 31:1233–1239.

Mao JR, Bristow J. 2001. The Ehlers–Danlos syndrome: on beyond collagens. J Clin Invest 107:1063–1069.

Miyake N, Kosho T, Mizumoto S, Furuichi T, Hatamochi A, Nagashima Y, Arai E, Takahashi K, Kawamura R, Wakui K, Takahashi J, Kato H, Yasui H, Ishida T, Ohashi H, Nishimura G, Shiina M, Saitsu H, Tsurusaki Y, Doi H, Fukushima Y, Ikegawa S, Yamada S, Sugahara K. Matsumoto N. 2010. Loss-of-function mutations of *CHST14* in a new type of Ehles–Danlos syndrome. Hum Mutat 31:966–974.

Schalkwijk J, Zweers MC, Steijlen PM, Dean WB, Taylor G, van Vlijmen IM, van Haren B, Miller WL, Bristow J. 2001. A recessive form of the Ehlers-Danlos syndrome caused by tenascin-X deficiency. N Engl J Med 345:1167–1175.

Schwarze U, Hata R, McKusick VA, Shinkai H, Hoyme HE, Pyeritz RE, Byers PH. 2004. Rare autosomal recessive cardiac valvular form of Ehlers-Danlos syndrome results from mutations in the COL1A2 gene that activate the nonsense-mediated RNA decay pathway. Am J Hum Genet 74:917–930.

Shimizu K, Okamoto N, Miyake N, Taira K, Sato Y, Matsuda K, Akimaru N, Ohashi H, Wakui K, Fukushima Y, Matsumoto N, Kosho T. 2011. Delineation of dermatan 4-O-sulfotransferase 1 deficient Ehlers-Danlos syndrome: observation of two additional patients and comprehensive review of 20 reported patients. Am J Med Genet Part A 155A:1949–1958.

Sonoda T, Kouno K. 2000. Two brothers with distal arthrogryposis, peculiar facial appearance, cleft palate, short stature, hydronephrosis, retentio testis, and normal intelligence: a new type of distal arthrogryposis? Am J Med Genet 91:280–285.

Steinmann B, Royce PM, Superti-Furga A. 2002. The Ehlers–Danlos syndrome. In: Royce PM, Steinmann B, editors. Connective tissue and its heritable disorders. New York: Wiley-Liss. p 431–523.

Voermans, NC, van Alfen N, Pillen S, Lammens M, Schalkwijk J, Zwarts MJ, van Rooij IA, Hamel BCJ, van Engelen BG. 2009. Neuromuscular involvement in various types of Ehlers–Danlos syndrome. Ann Neurol 65:687–697.

Yasui H, Adachi Y, Minami T, Ishida T, Kato Y, Imai K. 2003. Combination therapy of DDAVP and conjugated estrogens for a recurrent large subcutaneous hematoma in Ehlers–Danlos syndrome. Am J Hematol 72:71–72.

Zhang L, Müller T, Baenziger JU, Janecke AR. 2010. Congenital disorders of glycosylation with emphasis on loss of dermatan-4-sulfotransferase? 93:289–307.

Tomoki Kosho,[1]* Noriko Miyake,[2] Shuji Mizumoto,[3] Atsushi Hatamochi,[4] Yoshimitsu Fukushima,[1] Shuhei Yamada,[3] Kazuyuki Sugahara,[3] and Naomichi Matsumoto[2]

[1]Department of Medical Genetics, Shinshu University School of Medicine, Matsumoto, Japan; [2]Department of Human Genetics, Yokohama City University Graduate School of Medicine, Yokohama, Japan; [3]Laboratory of Proteoglycan Signaling and Therapeutics, Hokkaido University Graduate School of Life Science, Sapporo, Japan; [4]Department of Dermatology, Dokkyo Medical University, School of Medicine, Mibu, Japan

*Correspondence to: Tomoki Kosho, Department of Medical Genetics, Shinshu University School of Medicine, 3-1-1 Asahi, Matsumoto 390-8621, Japan. E-mail: ktomoki@shinshu-u.ac.jp

Received 9 April 2011; accepted revised manuscript 3 August 2011.
DOI: 10.1002/humu.21586, Published online 24 August 2011 in Wiley Online Library (www.wiley.com/humanmutation).

CLINICAL REPORT

AMERICAN JOURNAL OF medical genetics

A Homozygous Mutation in *RNU4ATAC* as a Cause of Microcephalic Osteodysplastic Primordial Dwarfism Type I (MOPD I) With Associated Pigmentary Disorder

Ghada M.H. Abdel-Salam,[1]* Noriko Miyake,[2] Maha M. Eid,[3] Mohamed S. Abdel-Hamid,[4] Nihal A. Hassan,[5] Ola M. Eid,[3] Laila K. Effat,[4] Tarek H. El-Badry,[6] Ghada Y. El-Kamah,[1] Mohamed El-Darouti,[7] and Naomichi Matsumoto[2]**

[1]Clinical Genetics Department, Human Genetics and Genome Research Division, National Research Centre, Cairo, Egypt

[2]Department of Human Genetics, Yokohama City University Graduate School of Medicine, Yokohama, Japan

[3]Human Cytogenetics Department, Human Genetics and Genome Research Division, National Research Centre, Cairo, Egypt

[4]Medical Molecular Genetics Department, Human Genetics and Genome Research Division, National Research Centre, Cairo, Egypt

[5]Ophthalmology Department, Faculty of Medicine, Cairo University, Cairo, Egypt

[6]Orodental Genetics Department, Human Genetics and Genome Research Division, National Research Centre, Cairo, Egypt

[7]Department of Dermatology, Faculty of Medicine, Cairo University, Cairo, Egypt

Received 3 July 2011; Accepted 17 August 2011

The designation microcephalic osteodysplastic primordial dwarfism (MOPD) refers to a group of autosomal recessive disorders, comprising microcephaly, growth retardation, and a skeletal dysplasia. The different types of MOPD have been delineated on the basis of clinical, radiological, and genetic criteria. We describe two brothers, born to healthy, consanguineous parents, with intrauterine and postnatal growth retardation, microcephaly with abnormal gyral pattern and partial agenesis of corpus callosum, and skeletal anomalies reminiscent of those described in MOPD type I. This was confirmed by the identification of the homozygous g.55G > A mutation of *RNU4ATAC* encoding U4atac snRNA. The sibs had yellowish-gray hair, fair skin, and deficient retinal pigmentation. Skin biopsy showed abnormal melanin function but *OCA* genes were normal. The older sib had an intracranial hemorrhage at 1 week after birth, the younger developed chilblains-like lesions at the age $2^1/_2$ years old but analysis of the *SAMHD1* and *TREX1* genes did not show any mutations. To the best of our knowledge, vasculopathy and pigmentary disorders have not been reported in MOPD I.

Key words: microcephalic osteodysplastic primordial dwarfism I (MOPD I); abnormal gyral pattern; pigmentary disorder; hypogenesis of corpus callosum; chilblains; fair skin; *U4atac snRNA*; vasculopathy; retinal pigmentation; microdontia

How to Cite this Article:
Abdel-Salam GMH, Miyake N, Eid MM, Abdel-Hamid MS, Hassan NA, Eid OM, Effat LK, El-Badry TH, El-Kamah GY, El-Darouti M, Matsumoto N. 2011. A homozygous mutation in *RNU4ATAC* as a cause of microcephalic osteodysplastic primordial dwarfism type I (MOPD I) with associated pigmentary disorder.
Am J Med Genet Part A 155:2885–2896.

INTRODUCTION

The term "microcephalic osteodysplastic primordial dwarfism" (MOPD) refers to the entities Seckel syndrome and microcephaly osteodysplastic primordial dwarfism (MOPD) type I/III and type II [Majewski et al., 1982; Meinecke and Passarge, 1991]. Variants of MOPD or Seckel-like syndrome have been described [Shebib et al., 1991; Buebel et al., 1996]. They share common findings such as severe intrauterine and postnatal growth retardation, microcephaly,

Additional supporting information may be found in the online version of this article.

*Correspondence to:
Ghada M.H. Abdel-Salam, Clinical Genetics Department, Human Genetics and Genome Research Division, National Research Centre, Tahrir Street, Dokki, Cairo, Egypt.
E-mail: ghada.abdelsalam@yahoo.com, ghasala@hotmail.com
**Correspondence to:
Naomichi Matsumoto, Department of Human Genetics, Yokohama City University Graduate School of Medicine, Yokohama, Japan.
E-mail: naomat@yokohama-cu.ac.jp

Published online 11 October 2011 in Wiley Online Library (wileyonlinelibrary.com).
DOI 10.1002/ajmg.a.34299

prominent nose, and micrognathia, but they have been delineated on the basis of specific clinical and radiological criteria. Recently, mutations of the *U4ATAC snRNA* gene were identified as a cause of MOPD I, while the *PCNT* gene was mutated in MOPD II and some Seckel syndrome patients [Griffith et al., 2008; Rauch et al., 2008; Edery et al., 2011; He et al., 2011]. Abnormalities of *CEP152* and *CENPJ* were found in other Seckel syndrome individuals [Al-Dosari et al., 2010].

MOPD I was first described by Taybi and Linder [1967] as cephaloskeletal dysplasia and fewer than 30 cases have been reported [Thomas and Nevin, 1976; Winter et al., 1985; Haan et al., 1989; Meinecke and Passarge, 1991; Meinecke et al., 1991; Eason et al., 1995; Berger et al., 1998; Sigaudy et al., 1998; Vichi et al., 2000; Klinge et al., 2002; Juric-Sekhar et al., 2011]. Skeletal findings in MOPD I include platyspondyly and vertebral clefting, horizontal acetabular roofs, elongated and curved clavicles, and short long bones with enlarged metaphyses including age-dependent bowing and undermodeled long bones. Malformations of the central nervous system have been reported such as migration disorders, partial or complete agenesis of the corpus callosum, hypoplastic frontal lobes, and vermis agenesis [Winter et al., 1985; Haan et al., 1989; Meinecke and Passarge, 1991; Meinecke et al., 1991; Klinge et al., 2002; Juric-Sekhar et al., 2011]. Congenital heart disease and renal tubular "leakage" were described in single cases [Eason et al., 1995; Sigaudy et al., 1998].

Recently, defects in a component of the minor spliceosome were identified in MOPD I. Mutations of *RNU4ATAC* encoding *U4atac snRNA* were found within the important structure known as the 5′ and 3′ stemloop, presumably disrupting snRNA's secondary structure leading to a <10% level of functional RNA [Edery et al., 2011; He et al., 2011; Heli et al., 2011]. The depletion of proteins specific to the U12-dependent spliceosome results in cellular growth arrest, thus severity of the minor spliceosome defects probably is transcript-specific [Edery et al., 2011; He et al., 2011].

We have studied two sibs with MOPD I associated with pigmentary disorder and vasculopathy. We present genetic analysis and clinical evaluation of this family.

CLINICAL REPORTS

Family History

The parents are healthy first cousins with unremarkable family history except for a paternal sister with short stature and delayed puberty (Fig. 1). Mother and father were 19 and 22 years old, respectively, at the time of birth of their first child. Parental height, weight and head circumference were on the 50th centile of both. The father had a normally pigmented skin, dark hair, and dark green iris color while the mother had fair skin, dark hair, and dark green iris color. Fundi of father were normal and mother had unilateral cataract and normal fundus pigmentation in the unaffected eye. Skin biopsy and ultrastructure study of the hairbulb melanocytes of the parents showed normal melanocyte and melanosome architecture. The parents have no normal children.

Patient 1

The male propositus was the first-born child of this family. He was preceded by a spontaneous abortion. Ultrasound scan in the 36th week of gestation showed intrauterine growth retardation with small biparietal diameter (BPD) and oligohydramnios. The boy was born at 39 weeks of gestation by cesarean section. Birth weight was 1,500 g (−3.7 SD); birth length and head circumference were not recorded. At the age of 1 week, weak cry, lethargy, and poor feeding were noticed. He was admitted to the hospital where brain CT scan showed fresh bleeding in the occipital region and falx cerebri. He was discharged after 7 days as his neurological examination results were normal and neither physical abnormalities nor seizures were noted. Complete blood picture, coagulation time and prothrombin time and concentration revealed normal results. We first saw the child at $2^1/_2$ years. On examination weight, length and head circumference were 7,000 g (−5.3 SD), 74.5 cm (−4.5 SD), and 37.5 cm (−8 SD), respectively. He had a (Fig. 2) fair complexion, sloping forehead, sparse eyebrows, large prominent eyes, nystagmus, prominent nose, flat philtrum, micrognathia, bilateral clinodactyly of 5th digits, dysplastic nails, knock knees, rocker-bottom feet, and normal toe nails.

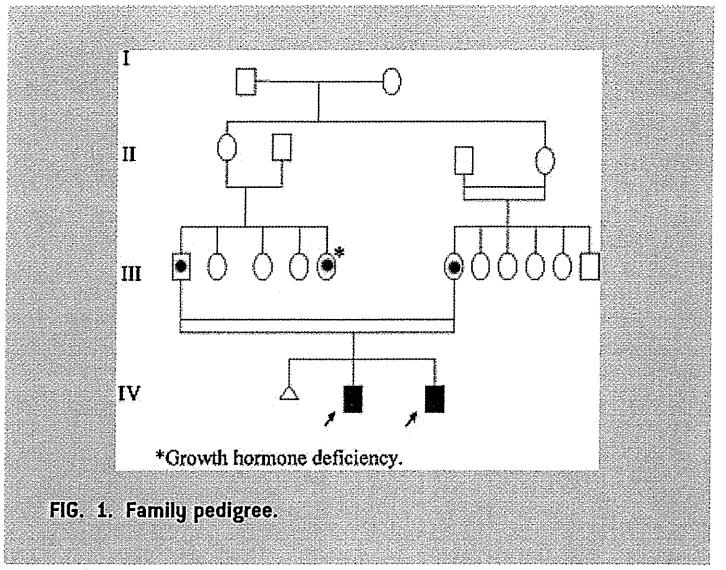

FIG. 1. Family pedigree.

Skeletal radiological examination (Fig. 3) of the pelvis at the age of 1 year showed horizontal acetabular roofs and unossified pubic bones. The femora appeared proportionately short. The metaphyses of the femora and tibiae were broad with irregular ends. The tibiae and fibulae were short and equal length.

At age 3 years, his weight, height and head circumference were 9,200 g (−3.4 SD), 79.5 cm (−3.8 SD), and 38.5 cm (−8.4 SD), respectively. He had a highly arched palate, multiple thick labial frenula, microdontia, enamel hypocalcification, and tooth caries with early loss of teeth (Fig. 1). Periapical radiographs of mandibular incisors showed normal roots of the erupted teeth. Psychomotor development was moderately delayed (he sat unsupported at 10 months, walked independently at 2 $^9/_{12}$ years, and had only a few words at 3 years). He had a cheerful personality.

At age 5 years, his weight, height and head circumference were 12 kg (−2.9 SD), 93 cm (−3.3 SD), and 39.5 cm (−9.1 SD), respectively. No history of repeated infections, eczema, or seizures had occurred until now.

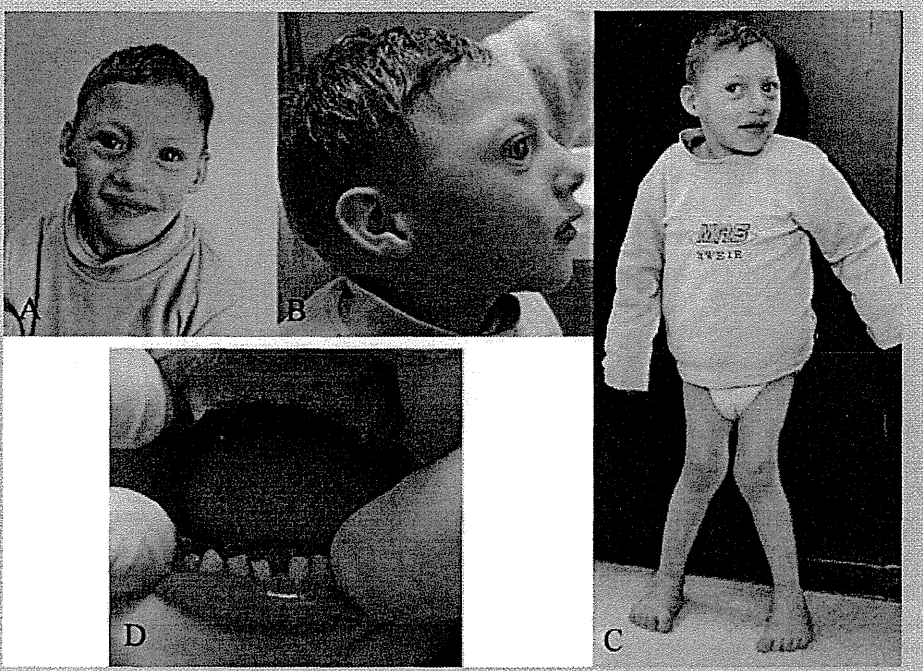

FIG. 2. Patient 1 at the age of 3 years. Note (A) large and prominent nose and fair color hair and skin. (B) Profile, (C) knock knees, (D) microdontia.

Laboratory studies documented iron deficiency anemia on several occasions. Results of leukocyte and platelet count, urine analysis, blood sugar, and metabolic screening were normal. Abdominal ultrasound findings were normal. Hearing on auditory brainstem response (ABR) was normal. His karyotype was 46, XY. Breakage analysis of 50 metaphases gave no evidence for excess spontaneous breakage. Fluorescent in situ hybridization (FISH) was performed to rule out the 15p and Xp22 deletions harboring the *OCA2* and *OCA1* genes, respectively, showed normal results.

EEG showed paroxysmal and generalized abnormal discharge of sharp and slow wave activity. Ophthalmological examinations showed blue and translucent irides and horizontal nystagmus. There was lack of fundal pigment without foveal landmarks.

Roentgenograms (Fig. 3) showed short long bones of the upper and lower limbs. Radii and ulnae appeared thin with a narrow medullary cavity. The femoral and proximal tibial metaphyses were slightly splayed and had an irregular margin. The fibulae were longer than the tibiae proximally. The iliac wings had an almost

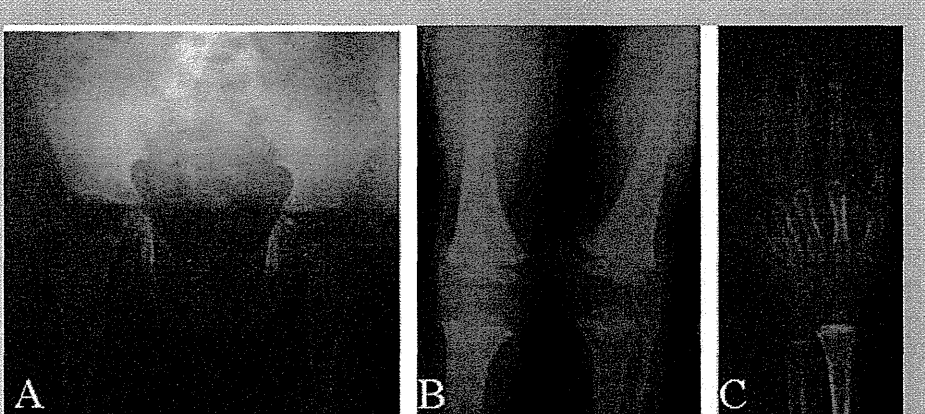

FIG. 3. Patient 1. A: Pelvis at the age of 1 year. The iliac wings have an almost normal configuration. The acetabular roofs are almost horizontal. The proximal femoral epiphysis are not ossified, the femoral necks are short and narrow. B: Knees. The distal metaphyses of the femora were flared and the distal femoral epiphyses were triangular in shape. C: Note short middle and distal phalanges, short first metacarpal bones.

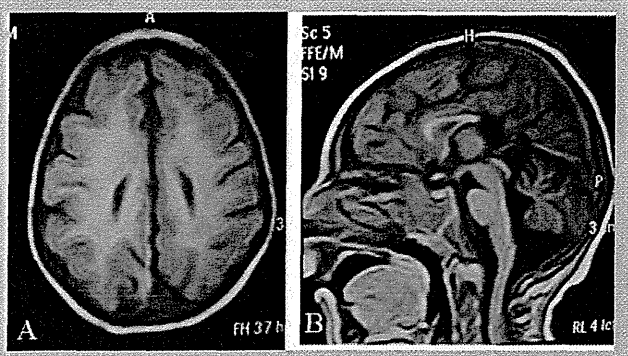

FIG. 4. Brain MRI of Patient 1 shows (A) axial T1-weighted image shows abnormal gyral pattern. B: Sagittal partial agenesis of corpus callosum especially the posterior part and hypoplasia of the vermis.

normal configuration and the acetabular roofs were still almost horizontal. The hands showed short metacarpals of the thumbs and the phalanges were short, particularly the middle and distal ones. Brain MRI (Fig. 4) at age 2 years showed abnormal gyral pattern, partial agenesis of corpus callosum and mild hypoplasia of the vermis.

The ultrastructure of the hair melanocytes showed normal melanocyte and melanosome architecture. There were no macromelanosomes. Incubation of hair bulbs was not done. Skin biopsy (Fig. 5) showed normal epidermis with no evidence of pigmentation. Melanosomes at the base of the epidermis were absent. Langerhans cells are seen at the upper part of the epidermis. Further, S-100 staining showed non-functioning melanocytes but Langerhans cells were stained.

Patient 2

He is the younger brother of Patient 1. Ultrasound scan in the 32nd week of gestation showed oligohydramnios and an inappropriately small baby with small BPD. He was born at 40 weeks of gestation by cesarean section. Birth weight was 1,850 g (−3.1 SD). Birth weight was 1,850 g (−3.1 SD). Birth length and head circumference were not recorded. Neonatal jaundice developed in the first few days of life. He was referred at age 2 months (Fig. 6). On examination weight, length, and head circumference were 2,750 g (−5.3 SD), 46 cm (−5.03 SD), and 30 cm (−6.25 SD), respectively. Fair skin was noticed as well as microcephaly, no scalp hair, sloping forehead, relatively large prominent nose, absent eyebrows, large prominent eyes, nystagmus, and micrognathia. His ears were small, posteriorly angulated, and apparently low set. His hands were small, the fingers were short and tapering and bilateral clinodactyly was also noticed. He had talipus varus equino feet and dysplatic toe nails. The skin was dry with cutis marmorata.

Neonatally, skull films (Fig. 7) showed small anterior fontanelle, dolicocephaly with prominent occiput and a small, receding forehead. On the chest radiographs, the ribs were narrow posteriorly and the anterior end was splayed. There was vertebral platyspondyly, cleft of cervical vertebrae and narrowing of the interpedicular distance especially in the cervical region. Ophthalmological examination documented identical findings to those of Patient 1 (transillumination of a blue iris, and lack of retinal pigment).

At age 8 months, weight, length, and head circumference were 5,750 g (−3 SD), 61 cm (−3.9 SD), and 36 (−6 SD), respectively. He had grayish, yellowish, sparse scalp hair, sparse eyebrows, flat philtrum, and micrognathia. He could sit unsupported. Dental examination at that time showed high palate, and multiple thick labial frenula but no eruption of teeth. Radiograph of the pelvis (Fig. 7) at that age showed normal configuration of the iliac wings, horizontal and smooth acetabular roofs. There was incomplete ossification of the pubic bones. The femoral necks were short and narrow. Femora had a thin cortex. At this age, brain MRI showed poorly developed gyri, agenesis of corpus callosum but brain structures in the posterior fossa appeared normally developed.

The patient was re-evaluated at age 1 year. At that time, his weight, length, and head circumference were 6 kg (−4.2 SD), 66 cm (−3.8 SD), and 37 cm (−6 SD), respectively. Dental examination showed that one of the lower incisors had erupted. The tooth was small with enamel hypocalcification. His development was mildly delayed, he was able to stand with support, grasped objects within

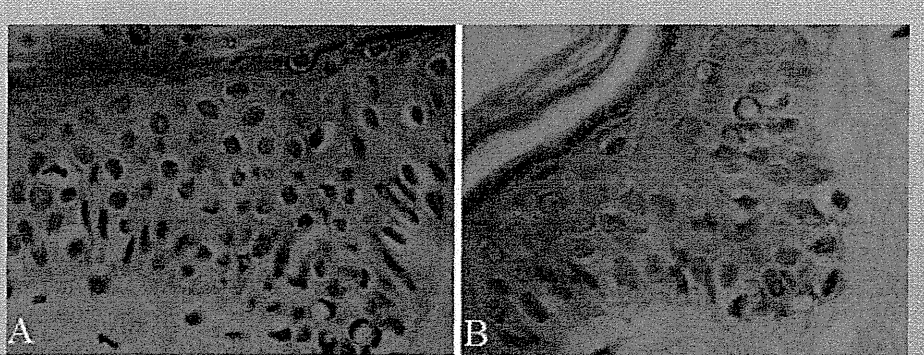

FIG. 5. Skin biopsy using (A) haematoxylin–eosin stain, original magnification 1,000× showed normally appearing epidermis with no evidence of pigmentation. Melanosomes at the base of the epidermis contain no melanosomes. Langerhans cells are seen at the upper part of the epidermis. B: S-100 staining showing non-functioning melanocytes. Langerhans cells are also positively stained (in the upper part of the epidermis).

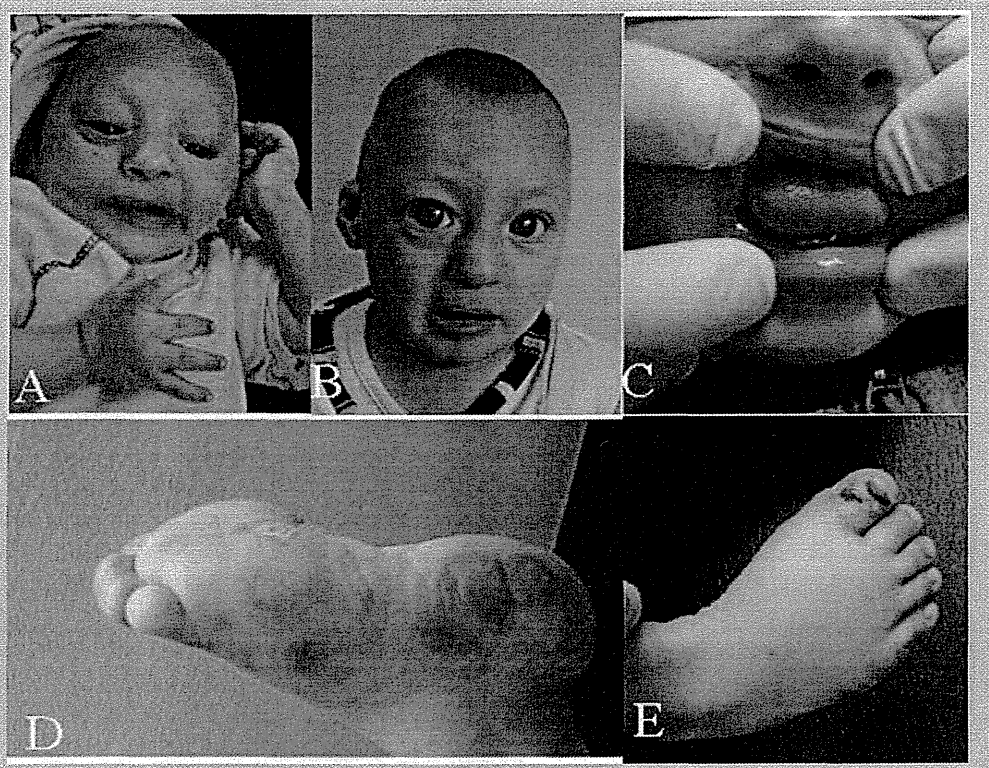

FIG. 6. Patient 2 at age of (A) 5 months, (B) 9 months. Note microcephaly with sloping forehead, dysmorphic ears, short limbs, hypotrichosis, and fair color of the skin. C: Bifid tip of the tongue. D: Chilblains like lesions on the sole. E: Necrotic lesions on the big toe.

reach and transferred them from one hand to the other and could vocalize one syllable sounds. Contact with family, environment and his behavior were normal for age. Chest roentgenogram (Fig. 7) showed increased thickness of the ribs. The clavicle appeared curved and elongated. The long bones of the upper limbs had a normal configuration. The hands showed short metacarpals of the thumbs and the phalanges were short. Fundus examination showed the same picture. He had repeated chest infections and was admitted to hospital. Further, he developed tonic–clonic convulsions (not related to fever) with good response to valproate.

Follow up at the age of $2^1/_2$ years showed weight, length, and head circumference: 7.750 kg (−3.5 SD), 77 cm (−3.8 SD), and 37.5 cm (−8.1 SD), respectively. Swollen reddish blue feet with acral eruptions on the soles (Fig. 6) were observed. These lesions were in the form of infiltrated, painful purplish papules. The big toe showed areas of necrosis with crust formation but no destruction of joints or gangrene formation. These skin lesions were exacerbated and recurrent in winter but usually resolve spontaneously within 3 weeks.

He had very dry skin on back and abdomen. He could stand with support and had started to communicate using few words. Ultrastructure of hair melanocytes was normal. There were no macromelanosomes. Incubation of hair bulbs was not done. Skin biopsy showed abnormal melanin function similar to that of his elder sib.

Urinary amino- and organic acids were normal. Studies of blood picture, immunoglobulins, antiphospholipid antibodies, and liver function tests gave normal results. Findings on abdominal ultrasonography, echo cardiography, and EEG were normal. Hearing on auditory brain response (ABR) was normal. His karyotype was 46, XY without any evidence for spontaneous excess breakage.

Patient 3

This 15-year-old girl is the youngest paternal aunt of Patients 1 and 2 and was referred for short stature and delayed puberty. The parents were non-consanguineous; the mother was 36 and the father 39 years old at the time of her birth. This was the fifth pregnancy; the other four pregnancies were normal but further information on birth weight, length, and head circumference were not available. On examination, her head circumference was 51.5 cm (−2.3 SD), height 143 cm (−3.15 SD), and weight 34 kg (−2.1 SD). Pubertal development was delayed. She had fair skin, deep green iris, and dark hair color. External genitalia were normal. She had no history of acrocyanosis, vasculitis, or seizures. IQ assessment (WISC-R) gave a score of 86. Hand films showed a delayed bone age. No skeletal changes were found in radiological assessment of long bones. Endocrine assessment showed growth hormone deficiency. Thyroid function, follicular stimulating hormone and

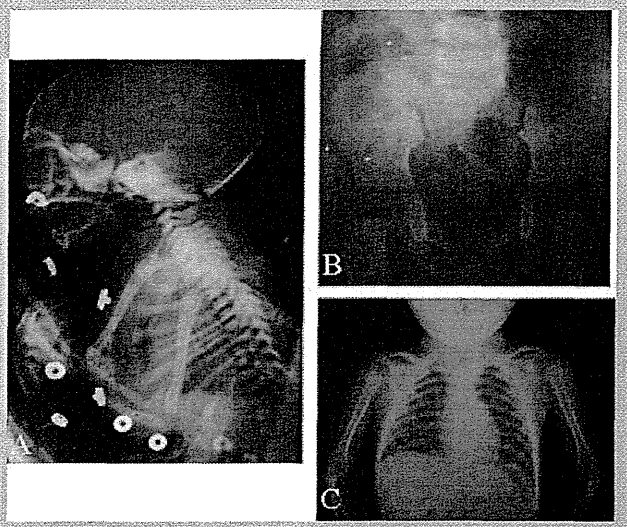

FIG. 7. X-ray of Patient 2 at birth. A: Skull. Note bathrocephaly and platyspondyly with coronal clefts of lumbar vertebral bodies. B: Pelvis at that age 7 months showed normal configuration of the iliac wings, horizontal and smooth acetabular roofs. There is incomplete ossification of the pubic bones. The femoral necks are short and narrow. Femur showed thin cortex. C: Chest at that age of 1 year showed increased thickness of the ribs. The clavicle appeared curved and elongated. The long bones of the upper limbs had normal configuration.

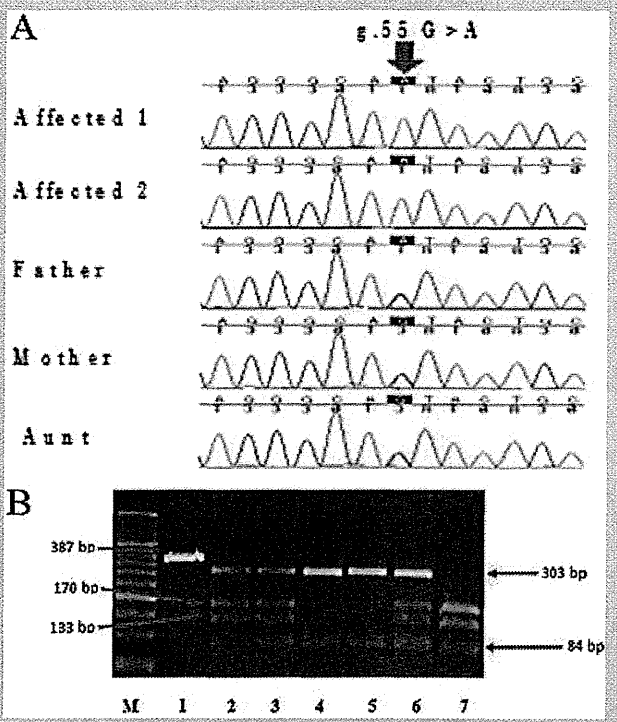

FIG. 8. Identification of g.55G > A mutation in the *RNU4ATAC* gene in our MOPD I family. A: Portion of the sequencing electropherogram showing the site of the mutation. B: PCR-RFLP analysis of the mutation using *TatI* restriction endonuclease (Thermo Fisher Scientific, Waltham, MA). Lane 1: Undigested PCR product. Lanes 2 and 3: father and mother heterozygous for the mutation. Lanes 4 and 5: the two patients. Lane 6: paternal aunt heterozygous for the mutation. Lane 7: normal control sample. M: 50 bp DNA Ladder (Thermo Fisher Scientific).

lutinizing hormone levels and blood picture were all normal. Abdomino-pelvic sonography showed normal prepubertal size of uterus and ovaries. Ophthalmic examination showed neither pendular nystagmus nor iris transillumination and fundus examination showed only some peripheral scattered areas of lack of pigmentation. Her karyotype was normal.

MUTATION ANALYSIS AND RESULTS

This research was reviewed and approved by the Research Ethics Committee of the National Research Centre according to "World Medical Association Declaration of Helsinki" and written informed consent was obtained.

Genomic DNA of our patients, their parents and the paternal aunt were screened for mutations in the *RNU4ATAC* gene in Yokohama City University. The gene and its flanking sequences were amplified by PCR and Sanger sequenced according to He et al. [2011]. Sequencing the *U4ATAC* gene showed a homozygous mutation g.55G > A in the two male sibs. The g.55G > A mutation was detected in the heterozygous state in the parents and the parental aunt using restriction fragment length polymorphism (RFLP) and was not found in 200 normal chromosomes of Egyptian origin (Fig. 8). Screening of the *OCA1, 2, 3, 4* genes was performed with normal results. In view of the chilblains skin lesions, screening of *TREX1* and *SAMHD1* genes was done in the Medical Molecular Genetics Department, National Research Centre, Egypt. These genes are the most commonly encountered with chilblains yet identified. The single exon of *TREX1* and 16 coding exons of *SAMHD1* and their flanking sequences were amplified by PCR and sequenced in both directions [Lee-Kirsch et al., 2007; Xin et al., 2011]. No pathogenic homozygous or heterozygous mutations were identified either in *TREX1* or *SAMHD1*.

DISCUSSION

These brothers had MOPD based on clinical and radiological findings. The radiological changes are diagnostic of MOPD I. Analysis of the recently discovered *U4ATAC* gene in MOPD I demonstrated the homozygous mutation (g.55G > A) similar to that found in the German MOPD I family described by He et al. [2011]. Thus, our patients have molecularly confirmed MOPD I with additional pigmentary changes which may either be newly observed manifestations of MOPD I or a coincidental finding, possibly due to homozygosity at another locus (F may be higher than 1/16 if ancestors were inbred). It was unexpected to find a heterozygous aunt with isolated growth hormone deficiency. Since the parents are clinically normal, the condition of the aunt probably does not represent heterozygosity of the MOPD I gene.

TABLE I. Summary of Clinical and Brain Imaging Features With or Without Mutation Analysis of Patients Reported With MOPD I Compared to Our Patients

Refs.	Cons	Sex	GA	BW	BL	BHC	CHD	Dry skin	External genitalia	Fundus	Brain imaging/ autopsy	Seizures/ EEG	Other findings	Survival	Cause of death	Mutational analysis
Taybi and Linder [1967], Patient 1		F	40 w	1,125 g	35 cm	25.5 cm	−	−	−	NA	ACC, AGP	−	−	22 d	Meconium peritonitis	NP
Taybi and Linder [1967], Patient 2	+	M	36 w	1,177 g	35 cm	24.5 cm	−	−	−	NA	ACC, AGP, enlarged lateral ventricles	−	−	1 y	Pneumonia	NP
Thomas and Nevin [1976], Patient 1		M	40 w	1,844 g	NA	NA	−	−	−	NA	NA	+	−	3 m	NA	NP
Thomas and Nevin [1976], Patient 2	−	M	29 w	1,955 g	NA	NA	−	−	−	NA	ACC	−	−	25 d	NA	NP
Majewski et al. [1982]	−	M	36 w	900 g	33 cm	24 cm	−	−	−	NA	NA	−	−	$3\frac{1}{2}$ m	NA	NP
Winter et al. [1985]	−	F	37 w	900 g	34 cm	24 cm	−	+	−	NA	Partial ACC, SGP	NA	−	1 y	Pyrexia of sepsis	NP
Haan et al. [1989] and He et al. [2011]	−	M	33 w	680 g	28 cm	23 cm	−	+	Undescended testes	Retinal dysplasia	ACC, AGP, CVH	NA	−	33 d	Fed inadequately	Homozygous g.51G > A
Meinecke and Passarge [1991], Patient 1	−	M	38 w	1,650 g	40 cm	27 cm	−	+	−	NA	NA	NA	−	$5\frac{1}{2}$ y	Pyrexia and vomiting	NP
Meinecke and Passarge [1991], Patient 2	−	F	40 w	1,400 g	36 cm	26 cm	−	+	Micro penis, undescended testes	NA	ACC, liss. of frontal lobe	Abnormal EEG	−	6 m	Sudden death	NP
Meinecke et al. [1991]	−	M	40 w	1,200 g	36 cm	27 cm	−	+	Undescended testes	NA	AGP, dilated lateral ventricles	NA	Proximal ureteral stenosis and hydronephrosis	$3\frac{1}{2}$ y	Chest infection	NP
Eason et al. [1995]	−	M	36 w	1,260 g	40 cm	27 cm	−	−	−	NA	AGP	+	Renal tubular leak of amino acids	5 m	Chest infection	NP

[*Continued*]

TABLE I. (*Continued*)

Refs.	Cons	Sex	GA	BW	BL	BHC	CHD	Dry skin	External genitalia	Fundus	Brain imaging/ autopsy	Seizures/ EEG	Other findings	Survival	Cause of death	Mutational analysis
Berger et al. [1998]	+	M	31 w	780 g	32 cm	21.7 cm	−	+	Undescended testes	NA	ACC, AGP, CVH	−	HSM and cholestasis, small kidneys	8 m	Sepsis	NP
Sigaudy et al. [1998], Patient 1	+	M	35 w	1,050 g	33 cm	24.5 cm	−	−	Undescended testes	NA	NA	−	−	4 m	Chest infection	NP
Sigaudy et al. [1998], Patient 2		M	39 w	765 g	29 cm	20 cm	−	−	Micro penis, undescended testes	NA	NA	−	−	Stillbirth	NA	NP
Sigaudy et al. [1998], Patient 3	−	F	21 w	150 g	19 cm	13 cm	ASD, coarctation of the aorta	−		NA	NA		Hypoplastic lungs and kidneys	TP	NA	NP
Sigaudy et al. [1998], Patient 4 and Edery et al. [2011], Family 3	+	F	39 w	1,415 g	33 cm	26 cm	−	+	Normal	NA	ACC, VA, CH	−	−	7 m	Frequent infection	Homozygous g.51G > A
Vichi et al. [2000], Patient 1	−	M	36 w	1,240 g	34 cm	24.5 cm	NA	+	Undescended testes	NA	ACC, AGP, IHC	−	−	4 y	Vomiting	NP
Vichi et al. [2000], Patient 2	−	M	36 w	1,350 g	NA	NA	NA	+	Micro penis, undescended testes	Unilateral cataract	ACC	−	−	$6\frac{1}{2}$ y	NA	NP
Klinge et al. [2002] and He et al. [2011]	−	M	33 w	1,060 g	34 cm	25 cm	−	+	Rt. Undescended testis	NA	HCC, AGP, CVH	−	Acute lymphatic leukemia	12 3/12 y	NA	Heterozygous g.30G >A and g.111G >A
Edery et al. [2011], Family 1, Patient 1	+	M	40 w	2,400 g	38.5 cm	32 cm	PFO	−	Micro penis, Lt. undescended testis	NA	ACC, NMD, brain cyst	−	−	11 m	Gastroenteritis	Homozygous g.51G > A
Edery et al. [2011], Family 1, Patient 2	+	M	$37\frac{1}{2}$ w	2,230 g	39 cm	30.5 cm	−	+	−	NA	ACC, microlissencephaly	+	−	10 m	Gastroenteritis	Homozygous g.51G > A
Edery et al. [2011], Family 2	+	F	38 w	1,060 g	31 cm	23.4 cm	VSD	−	−	NA	ACC, microlissencephaly	−	Polycystic kidney	14 m	After episodes of pyrexia	Homozygous g.51G > A

(*Continued*)

TABLE I. (*Continued*)

Refs.	Cons	Sex	GA	BW	BL	BHC	CHD	Dry skin	External genitalia	Fundus	Brain imaging/ autopsy	Seizures/ EEG	Other findings	Survival	Cause of death	Mutational analysis
Edery et al. [2011], Family 4; Patient 1		F	39 w	1,620 g	38 cm	25.5 cm	–	–	–	NA	ACC, AGP	–	–	1 m	Frequent infection	Homozygous g.51G > A
Edery et al. [2011], Family 4; Patient 2	+	F	40 w	1,580 g	37 cm	26 cm	–	–	–	NA	ACC, AGP, CVH	+	–	28 m	Frequent infection	Homozygous g.51G > A
Edery et al. [2011], Family 4; Patient 3		M	TP	NA	NA	NA	NA	NA	NA	NA	NA	NA	NA	NA	NA	Homozygous g.51G > A
Edery et al. [2011], Family 5	–	M	?	1,300 g	37.5 cm	27 cm	–	–	–	–	ACC, PMG	NA	Preaxial polydactyly hypoplastic thumb	NA	NA	Homozygous g.51G > A
Edery et al. [2011], Family 6	–	M	36 w	1,195 g	35 cm	24.5 cm	–	–	–	–	ACC, PMG, poorly developed ventricular system	–	–	6 m	NA	Heterozygous g.50G > A and g.51G > A
Edery et al. [2011], Family 7	–	F	32 w	658 g	28 cm	22.5 cm	ASD	+	–	NA	ACC, dilated lateral ventricles, thin brain mantle	–	GER	28 m	NA	Heterozygous g.51G > A and g.53G > A
Edery et al. [2011], Family 8	–	F	TP at 15 w	NA	NA	NA	NA	NA	–	NA	HCC, IHC, PMG	NA	NA	NA	NA	Heterozygous g.51G > A and g.53G > A
Juric-Sekhar et al. [2011]	–	F	34 w	990 g	33 cm	25 cm	PDA	–	–	Retinopathy of prematurity	ACC, liss., IHC	+	Hypoplastic thumb and distal phalanges, GER, inguinal hernia	11 m	NA	NP
Present study, Patient 1		M	39 w	1,500 g	NA	NA	–	–	–	Lack of fundal pigments	HCC, AGP, CVH	Abnormal EEG	Cutaneous albinism	Still alive	NA	Homozygous g.55G > A

(*Continued*)

TABLE I. (Continued)

Refs.	Cons	Sex	GA	BW	BL	BHC	CHD	Dry skin	External genitalia	Fundus	Brain imaging/ autopsy	Seizures/ EEG	Other findings	Survival	Cause of death	Mutational analysis
Present study, Patient 2	+	M	40 w	1,850 g	NA	NA	−	+	−	Lack of fundal pigments	ACC, AGP	+	Cutaneous albinism, chilblains like lesions	Still alive	NA	Homozygous g.55G>A

ACC, agenesis of corpus callosum; AGP, abnormal gyral pattern; ASD, atrial septal defect; BW, birth weight; BL, birth length; BHC, birth head circumference; CHD, congenital heart disease; cons, consanguinity; CVH, cerebellar vermis hypoplasia; F, female; GA, gestational age; GER, gastro-esophageal reflux; HCC, hypogenesis of corps callosum; liss., lissencephaly; PMG, polymicrogyri; SGP, simplified gyral pattern; IHC, interhemispheric cyst; VA, vermal atrophy; CH, cerebellar hypoplasia; HSM, hepatosplenomegaly; M, male; NA, not available; NP, not performed; PDA, patent ductus arteriosus; PFO, patent foramen ovale; TP, terminated pregnancy; VSD, ventricular septal defect.

Pigmentary changes have not been reported in MOPD I. Café-au-lait spots, freckling, dark pigmentation around the neck, on the trunk and in the axilla, hypopigmentation and poikiloderma were described only in MOPD II [Kantaputra et al., 2004; Webber et al., 2008]. While in Seckel syndrome, few patients show streaks of brown pigmentation in the neck, groins, and axillae and diffuse hypopigmented macules and papules were described before [Brackeen et al., 2007]. Our patients had fair skin color and hair and skin biopsy showed decreased function of the melanocytes. In addition, they had chorioretinal hypopigmentation in the absence of other ocular abnormalities, such as misrouting of the optic nerve fibers. The retinal changes observed in our patients do not indicate a specific retinal disorder but are like those associated with albinism. Thus, we considered one of the oculocutaneous albinism syndromes, but this diagnosis was ruled out after molecular testing. Pigmentary retinopathy has in fact been reported in patients with MOPD II and Seckel syndrome [Guirgis et al., 2001; Maclean et al., 2002].

Cataract is another finding described in MOPD I [Vichi et al., 2000] and atypical patients with MOPD II [Toriello et al., 1986; Hersh et al., 1994]. The mother of the two sibs had a unilateral cataract. It is unknown whether this condition could be due to the carrier status of the recessive gene.

We are aware of the reported Spanish patients with severe microcephaly, oculocutaneous albinism, hypogenesis of corpus callosum, and hypoplasia of the distal digital phalanges [Castro-Gago et al., 1983]. However, our patients did not show distal phalangeal deficiency.

Abnormalities of CNS vessels or vasculopathy are common in MOPD II patients, less common in Seckel syndrome manifested as cerebral aneurysms, tortuous vessels or moyamoya disease leading to life threatening CNS hemorrhages and strokes in early life [D'Angelo et al., 1998; Nishimura et al., 2003; Brancati et al., 2005; Bober et al., 2010] but never described in MOPD I. Patient 1 had intracranial hemorrhage at the age of 1 week that resolved spontaneously thereafter. A bleed in the occipital region/posterior falx as in Patient 1 may represent birth trauma to cavernous sinus. No other bleeding manifestations occurred in the sibs postnatally.

We were intrigued by the observation of acrocyanosis and the chilblain lesions in the younger brother that developed at the age of $2^1/_2$ years. These events might be a reflection of pathological vascular changes in specific organs/tissues. Nevertheless, the normal results of *SAMHD1* and *TREX1* sequencing in our patients led us to speculate that *RNU4ATAC* may play an important role in cerebral and even skin vasculopathy, and further studies of the role of *RNU4ATAC* in blood vessel integrity will be very important.

More generally, we ruled other conditions associated with chilblains like lesions such as antiphospholipid syndrome, neonatal systemic lupus or Aicardi–Goutières syndrome seem unlikely to be relevant from a clinical or pathogenic viewpoint.

We would like to highlight the oro-dental anomalies found in our MOPD I patients that have not been discussed before probably due to the early lethality of these cases. The two sibs reported here had microdontia and enamel hypocalcification. In another word, the teeth appeared proportionate to their dental arches and overall body size. Compared to MOPD II, microdontia in both dentitions, bulbous crowns, hypoplastic alveolar processes, opalescent teeth,

and short roots were reported [Kantaputra et al., 2004, 2011]. In Seckel syndrome, tooth anomalies include atrophic or absent teeth, macrodontia, hypoplasia of enamel, overcrowded and short roots [Thompson and Pembrey, 1985; Kjaer et al., 2001].

There was phenotypic variability between the two sibs (Table I). Although the eldest boy had normal skin, no seizures, hypoplastic cerebellar vermis and could walk, talk, and repeat short sentences, his younger sib had very dry, hyperkeratotic skin, seizures, normal cerebellum and could not walk or talk. This phenotypic variability strongly suggests a significant role for splicing of various functional genes relevant to corresponding phenotypes [Wang and Cooper, 2007; Graveley, 2008]. Further characterization of distinct mutations in *RNU4ATAC* will shed light on some of these difficulties of clinical classification.

The growth pattern of the two sibs revealed interesting results showing very severe growth retardation in the infantile period but some improvement in the weight and length thereafter in spite of the continuous deceleration head circumference.

Compared to MOPD II and Seckel syndrome, MOPD I has poor prognosis. Death usually occurs in the first year of life due to infectious diseases and rarely in early childhood (Table I). Also of interest is the unusually long survival of the first patient reported here for more than 5 years.

In conclusion, we describe unexpected findings of pigmentation disorders and vasculopathy in two sibs with MOPD I syndrome. We could not draw any firm conclusion on the relationship between the RNU4ATAC mutation and the pigmentation disorder and chilblains like lesions in our two patients. There could be a causal variant not genotyped in this study that is responsible for these traits. In the mean time, the recurrence of these traits in the two sibs led us to suggest that this mutation may contribute to the association of pigmentation disorder and vasculopathy. Further studies of MOPD I patients are absolutely necessary to determine the true prevalence of the reported abnormalities.

REFERENCES

Al-Dosari MS, Shaheen R, Colak D, Alkuraya FS. 2010. Novel *CENPJ* mutation causes Seckel syndrome. J Med Genet 47:411–414.

Berger A, Haschke N, Kohlhauser C, Amman G, Unterberger U, Weninger M. 1998. Neonatal cholestasis and focal medullary dysplasia of the kidneys in a case of microcephalic osteodysplastic primordial dwarfism. J Med Genet 35:61–64.

Bober MB, Khan N, Kaplan J, Lewis K, Feinstein JA, Scott CI Jr, Steinberg GK. 2010. Majewski osteodysplastic primordial dwarfism type II (MOPD II): Expanding the vascular phenotype. Am J Med Genet Part A 152A:960–965.

Brackeen A, Babb-Tarbox M, Smith J. 2007. Pigmentary changes and atopic dermatitis in a patient with Seckel syndrome. Pediatr Dermatol 24:53–56.

Brancati F, Castori M, Mingarelli R, Dallapiccola B. 2005. Majewski osteodysplastic primordial dwarfism type II (MOPD II) complicated by stroke: Clinical report and review of cerebral vascular anomalies. Am J Med Genet Part A 139A:212–215.

Buebel MS, Salinsas CF, Pai GS, Macpherson RI, Greer MK, Perez-Comas A. 1996. A new Seckel-like syndrome of primordial dwarfism. Am J Med Genet 64:447–452.

Castro-Gago M, Pombo M, Novo I, Tojo R, Pena J. 1983. Syndrome familiar de microcefalia con albinismo oculocutaneo y anomalies digitales. Ann Esp Pediatr 19:128–131.

D'Angelo VA, Ceddia AM, Zelante L, Florio FP. 1998. Multiple intracranial aneurysms in a patient with Seckel syndrome. Childs Nerv Syst 14:82–84.

Eason J, Hall CM, Trounce JQ. 1995. Renal tubular leakage complicating microcephalic osteodysplastic primordial dwarfism. J Med Genet 32: 234–235.

Edery P, Marcaillou C, Sahbatou M, Labalme A, Chastang J, Touraine R, Tubacher E, Senni F, Bober MB, Nampoothiri S, Jouk P-S, Steichen E, Berland S, Toutain A, Wise CA, Sanlaville D, Rousseau F, Clerget-Darpoux F, Leutenegger AL. 2011. Association of TALS developmental disorder with defect in minors splicing component *U4ATAC* snRNA. Science 332:240–243.

Griffith E, Walker S, Martin CA, Vagnarelli P, Stiff T, Vernay B, Al Sanna N, Saggar A, Hamel B, Earnshaw WC, Jeggo PA, Jackson AP, O'Driscoll M. 2008. Mutations in pericentrin cause Seckel syndrome with defective ATR-dependent DNA damage signaling. Nat Genet 40:232–236.

Graveley BR. 2008. The haplo-spliceo-transcriptome: Common variations in alternative splicing in the human population. Trends Genet 24:5–7.

Guirgis MF, Lam BL, Howard CW. 2001. Ocular manifestations of Seckel syndrome. Am J Ophthalmol 132:596–597.

Haan EA, Furness ME, Knowles S, Morris LL, Scott G, Svigos JM, Vigneswaren R. 1989. Osteodysplastic primordial dwarfism: Report of a further case with manifestations similar to those of types I and III. Am J Med Genet 33:224–227.

He H, Liyanarachchi S, Akagi K, Nagy R, Li J, Dietrich RC, Li W, Sebastian N, Wen B, Xin B, Singh J, Yan P, Alder H, Haan E, Wieczorek D, Albrecht B, Puffenberger E, Wang H, Westman JA, Padgett RA, Symer DE, de la Chapelle A. 2011. Mutations in *U4ATAC* snRNA, a component of the minor spliceosome, in the developmental disorder MOPD I. Science 332: 238–240.

Heli K, Pessa J, Frilander MJ. 2011. Minor splicing, disrupted. Science 332:184–185.

Hersh JH, Joyce MR, Spranger J, Goatley EC, Lachman RS, Bhatt S, Rimoin DL. 1994. Microcephalic oseteodysplastic dysplasia. Am J Med Genet 51:194–199.

Juric-Sekhar G, Kapur RP, Glass IA, Murray ML, Parnell SE, Hevner RF. 2011. Neuronal migration disorders in microcephalic osteodysplastic primordial dwarfism type I/III. Acta Neuropathol 121:545–554.

Kantaputra PN, Tanpaiboon P, Unachak K, Praphanphoj V. 2004. Microcephalic osteodysplastic primordial dwarfism with severe microdontia and skin anomalies: Confirmation of a new syndrome. Am J Med Genet Part A 130A:181–190.

Kantaputra P, Tanpaiboon P, Porntaveetus T, Ohazama A, Sharpe P, Rauch A, Hussadaloy A, Thiel CT. 2011. The smallest teeth in the world are caused by mutations in the *PCNT* gene. Am J Med Genet Part A 155A: 1398–1403.

Kjaer I, Hansen N, Becktor KB, Birkebaek N, Balslev T. 2001. Craniofacial morphology, dentition, and skeletal maturity in four siblings with Seckel syndrome. Cleft Palate Craniofac J 38:645–651.

Klinge L, Schaper J, Wieczorek D, Voit T. 2002. Microlissencephaly in microcephalic osteodysplastic primordial dwarfism: A case report and review of the literature. Neuropediatrics 33:309–313.

Lee-Kirsch MA, Chowdhury D, Harvey S, Gong M, Senenko L, Engel K, Pfeiffer C, Hollis T, Gahr M, Perrino FW, Lieberman J, Hubner N. 2007. A mutation in *TREX1* that impairs susceptibility to granzyme A-mediated cell death underlies familial chilblain lupus. J Mol Med 85:531–537.

Maclean K, Amblerb G, Flahertyc M, Kozlowskid K, Adès LC. 2002. A variant microcephalic osteodysplastic slender bone disorder with growth hormone deficiency and a pigmentary retinopathy. Clin Dysmorphol 11:255–260.

Majewski F, Stoeckenius M, Kemperdick H. 1982. Studies of microcephalic primordial dwarfism III: An intrauterine dwarf with platyspondyly and anomalies of pelvis and clavicles: Osteodysplastic primordial dwarfism type III. Am J Med Genet 12:37–42.

Meinecke P, Passarge E. 1991. Microcephalic osteodysplastic primordial dwarfism type I/III in sibs. J Med Genet 28:795–800.

Meinecke P, Schaefer E, Wiedemann HR. 1991. Microcephalic osteodysplastic primordial dwarfism: Further evidence for identity of the so-called types I and III. Am J Med Genet 39:232–236.

Nishimura G, Hasegawa T, Fujno M, Hoi N, Tomitas Y. 2003. Microcephalic osteodysplastic primordial short stature type II with café-au-lait spots and moyamoya disease. Am J Med Genet Part A 117A:299–301.

Rauch A, Thiel CT, Schindler D, Wick U, Crow YJ, Ekici AB, van Essen AJ, Goecke TO, Al-Gazali L, Chrzanowska KH, Zweier C, Brunner HG, Becker K, Curry CJ, Dallapiccola B, Devriendt K, Dőrfler A, Kinning E, Megarbane A, Meinecke P, Semple RK, Spranger S, Toutain A, Trembath RC, Voss E, Wilson L, Hennekam R, de Zegher F, Dőrr HG, Reis A. 2008. Mutations in the pericentrin (*PCNT*) gene cause primordial dwarfism. Science 319:816–819.

Shebib S, Hugosson C, Sakati N, Nyhan WL. 1991. Osteodysplastic variant of primordial dwarfism. Am J Med Genet 40:146–150.

Sigaudy S, Toutain A, Moncla A, Fredouille C, Bourliere B, Aymé S, Philip N. 1998. Microcephalic osteodysplastic primordial dwarfism Taybi-Linder type: Report of four cases and review of the literature. Am J Med Genet 80:16–24.

Taybi H, Linder D. 1967. Congenital familial dwarfism with cephaloskeletal dysplasia. Radiology 89:275–281.

Thomas PS, Nevin NC. 1976. Congenital familial dwarfism with cephaloskeletal dysplasia. Ann Radiol 19:187–192.

Thompson E, Pembrey M. 1985. Seckel syndrome: An overdiagnosed syndrome. J Med Genet 22:192–201.

Toriello HV, Horton WA, Oostendorp A, Waterman DF, Higgins JV. 1986. An apparently microcephalic primordial dwarfism and cataracts. Am J Med Genet 25:1–8.

Vichi GF, Currarino G, Wasserman RL, Duvina PL, Filippi L. 2000. Cephaloskeletal dysplasia (Taybi-Linder syndrome; osteodysplastic dwarfism type III): Report of two cases and review of the literature. Pediatr Radiol 30:644–652.

Wang GS, Cooper TA. 2007. Splicing in disease: Disruption of the splicing code and the decoding machinery. Nat Rev Genet 8:749–761.

Webber N, O'toole EA, Paige DG, Rosser E. 2008. Cutaneous features associated with microcephalic osteodysplastic primordial dwarfism type II. Pediatr Dermatol 25:401–402.

Winter RM, Wigglesworth J, Harding BN. 1985. Osteodysplastic dwarfism: Report of a further patient with manifestations similar to those seen in patients with types I and III. Am J Med Genet 21:569–574.

Xin B, Jones S, Puffenberger EG, Hinze C, Bright A, Tan H, Zhou A, Wu G, Vargus-Adams J, Agamanolis D, Wang H. 2011. Homozygous mutation in *SAMHD1* gene causes cerebral vasculopathy and early onset stroke. Proc Natl Acad Sci USA 108:5372–5377.

REPORT

Mutations in *POLR3A* and *POLR3B* Encoding RNA Polymerase III Subunits Cause an Autosomal-Recessive Hypomyelinating Leukoencephalopathy

Hirotomo Saitsu,[1,*] Hitoshi Osaka,[2] Masayuki Sasaki,[3] Jun-ichi Takanashi,[4] Keisuke Hamada,[5] Akio Yamashita,[6] Hidehiro Shibayama,[7] Masaaki Shiina,[5] Yukiko Kondo,[1] Kiyomi Nishiyama,[1] Yoshinori Tsurusaki,[1] Noriko Miyake,[1] Hiroshi Doi,[1] Kazuhiro Ogata,[5] Ken Inoue,[8] and Naomichi Matsumoto[1,*]

Congenital hypomyelinating disorders are a heterogeneous group of inherited leukoencephalopathies characterized by abnormal myelin formation. We have recently reported a hypomyelinating syndrome characterized by diffuse cerebral hypomyelination with cerebellar atrophy and hypoplasia of the corpus callosum (HCAHC). We performed whole-exome sequencing of three unrelated individuals with HCAHC and identified compound heterozygous mutations in *POLR3B* in two individuals. The mutations include a nonsense mutation, a splice-site mutation, and two missense mutations at evolutionally conserved amino acids. Using reverse transcription-PCR and sequencing, we demonstrated that the splice-site mutation caused deletion of exon 18 from *POLR3B* mRNA and that the transcript harboring the nonsense mutation underwent nonsense-mediated mRNA decay. We also identified compound heterozygous missense mutations in *POLR3A* in the remaining individual. *POLR3A* and *POLR3B* encode the largest and second largest subunits of RNA Polymerase III (Pol III), RPC1 and RPC2, respectively. RPC1 and RPC2 together form the active center of the polymerase and contribute to the catalytic activity of the polymerase. Pol III is involved in the transcription of small noncoding RNAs, such as 5S ribosomal RNA and all transfer RNAs (tRNA). We hypothesize that perturbation of Pol III target transcription, especially of tRNAs, could be a common pathological mechanism underlying *POLR3A* and *POLR3B* mutations.

Congenital hypomyelinating disorders form a heterogeneous group of central nervous system leukoencephalopathies that is characterized by abnormal myelin formation. Although these conditions are readily recognized by brain magnetic resonance imaging (MRI), many cases are not diagnosed correctly.[1] Several syndromes affecting myelination, such as hypomyelination with hypodontia and hypogonadotropic hypogonadism (4H) syndrome (MIM 612440) and hypomyelination with atrophy of the basal ganglia and cerebellum (H-ABC) (MIM 612438), have been described.[2–5] We have recently reported a hypomyelinating syndrome characterized by diffuse cerebral hypomyelination with cerebellar atrophy and hypoplasia of the corpus callosum (HCAHC).[6] Individuals with HCAHC do not show hypodontia or atrophy of the basal ganglia, which are observed in 4H syndrome and H-ABC; however, diffuse hypomyelination, atrophy, or hypoplasia of the cerebellum and corpus callosum are overlapping features of these three syndromes, suggesting that there might be a common underlying pathological mechanism.

Here, we report on four individuals with HCAHC from three unrelated families (Figure 1A; Table 1). Clinical information and peripheral blood or saliva samples were obtained from the family members after obtaining written informed consent. Experimental protocols were approved by the Institutional Review Board of Yokohama City University. To identify pathogenic mutations, we performed whole-exome sequencing of three probands from three unrelated families (individuals 1, 3, and 4). DNAs were captured with the SureSelect Human All Exon 50Mb Kit (Agilent Technologies, Santa Clara, CA) and sequenced with one lane per sample on an Illumina GAIIx (Illumina, San Diego, CA) with 108 bp paired-end reads. Image analysis and base calling were performed by sequence control software real-time analysis and CASAVA software v1.7 (Illumina). A total of 90,014,368 (individual 1), 86,942,264 (individual 3), and 92,168,758 (individual 4) paired-end reads were obtained and aligned to the human reference genome sequence (GRCh37/hg19) with MAQ[7] and NextGENe software v2.00 with sequence condensation by consolidation (SoftGenetics, State College, PA). This approach resulted in more than 88% of target exomes being covered by ten reads or more (see Table S1, available online). Single nucleotide variants (SNVs) were called with MAQ and NextGENe. Small insertions and deletions were

[1]Department of Human Genetics, Yokohama City University Graduate School of Medicine, 3-9 Fukuura, Kanazawa-ku, Yokohama 236-0004, Japan; [2]Division of Neurology, Clinical Research Institute, Kanagawa Children's Medical Center, 2-138-4 Mutsukawa, Minami-ku, Yokohama 232-8555, Japan; [3]Department of Child Neurology, National Center of Neurology and Psychiatry, 4-1-1 Ogawahigashi-cho Kodaira, Tokyo 187-8551, Japan; [4]Department of Pediatrics, Kameda Medical Center, 929 Higashi-cho, Kamogawa-shi, Chiba 296-8602, Japan; [5]Department of Biochemistry, Yokohama City University Graduate School of Medicine, 3-9 Fukuura, Kanazawa-ku, Yokohama 236-0004, Japan; [6]Department of Molecular Biology, Yokohama City University Graduate School of Medicine, 3-9 Fukuura, Kanazawa-ku, Yokohama 236-0004, Japan; [7]Department of Neurology, Kameda Medical Center, 929 Higashi-cho, Kamogawa-shi, Chiba 296-8602, Japan; [8]Department of Mental Retardation and Birth Defect Research, National Institute of Neuroscience, National Center of Neurology and Psychiatry, 4-1-1 Ogawahigashi-cho Kodaira, Tokyo 187-8551, Japan
*Correspondence: hsaitsu@yokohama-cu.ac.jp (H.S.), naomat@yokohama-cu.ac.jp (N.M.)
DOI 10.1016/j.ajhg.2011.10.003.

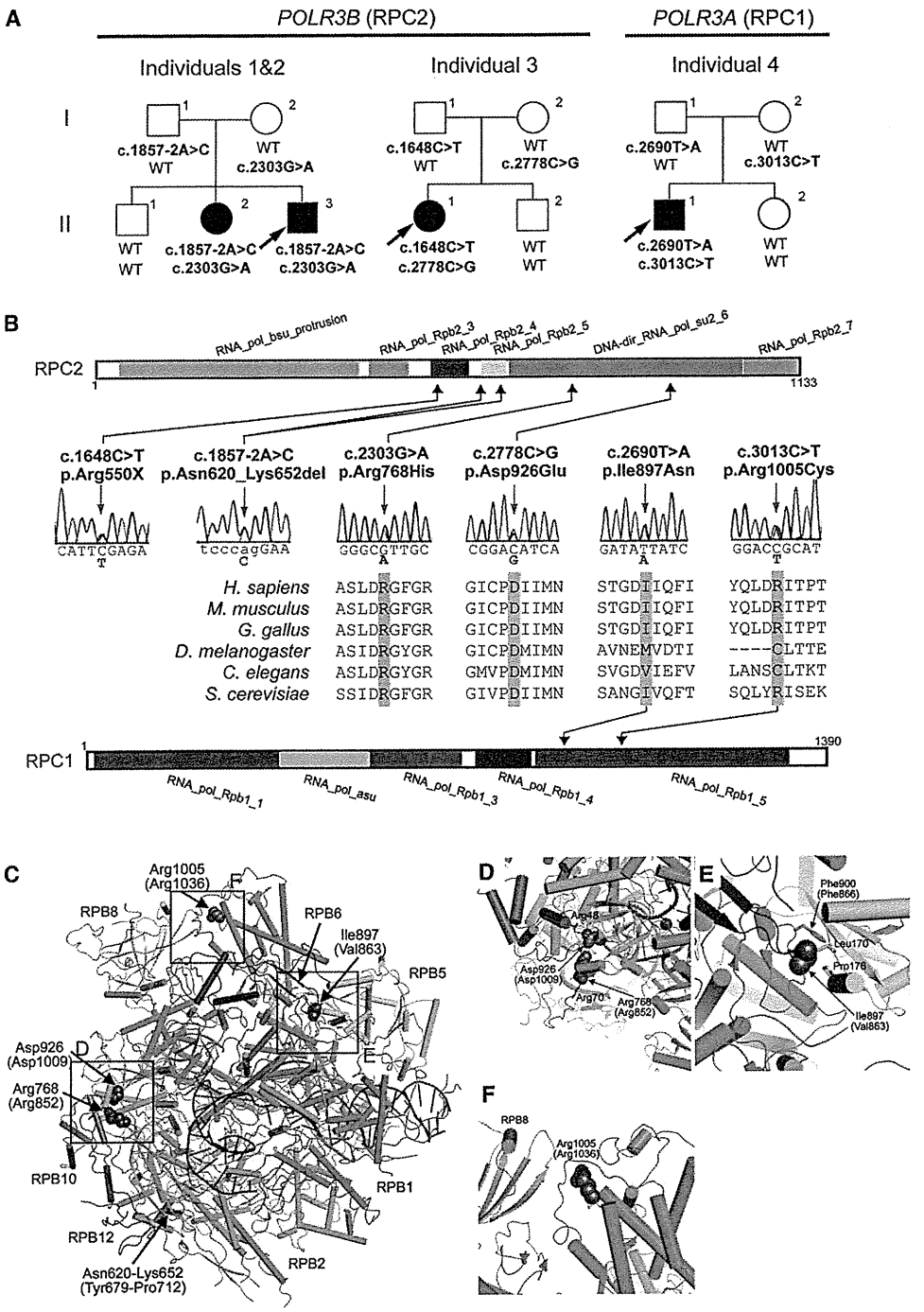

Figure 1. Mutations in *POLR3B* and *POLR3A*

(A) Pedigrees of four kindreds with HCAHC are shown. We identified four mutations in *POLR3B* encoding RPC2 in three individuals from two unrelated families and two mutations in *POLR3A* encoding RPC1 in one family. The segregation of each mutation is shown.

(B) Schematic representation of RPC2 (upper) and RPC1 (lower) proteins with Pfam domains (from Ensembl). Locations of each amino-acid-altering mutation are depicted with electropherograms. All of the missense mutations occurred at evolutionally conserved amino acids. Homologous sequences were aligned with the CLUSTALW website.

(C–F) 3D representations of RPC1 and RPC2 mutations. Mutated amino acids in RPC1 and RPC2 are shown along with their equivalent positions in the homologous RPB1 and RPB2 subunits of RNA Polymerase II (amino acid and its position in parenthesis). The structure and positions of mutations are illustrated by PyMOL with the crystal structure (PDB accession number 3GTP). RPB3, RPB9, and RPB11 subunits, which are specific to RNA Polymerase II, have been omitted from the figure. RPB1 is shown in green, RPB2 in sky blue, RPB5 in yellow, RPB6 in dark blue, RPB8 in pink, RPB10 in orange, RPB12 in purple, DNA in brown, and RNA in red. Amino acids that interact with mutated amino acids are also shown.

Table 1. Clinical Features of the Individuals

Clinical Features	Individual 1	Individual 2	Individual 3	Individual 4
Genes	*POLR3B*	*POLR3B*	*POLR3B*	*POLR3A*
Mutations, DNA	c.1857-2A>C, c.2303G>A	c.1857-2A>C, c.2303G>A	c.1648C>T, c.2778C>G	c.2690T>A, c.3013C>T
Mutations, protein	p.Asn620_Lys652del, p.Arg768His	p.Asn620_Lys652del, p.Arg768His	p.Arg550X, p.Asp926Glu	p.Ile897Asn, p.Arg1005Cys
Gender	M	F	F	M
Current age (years)	27	30	16	17
Intellectual disability	mild	mild	moderate	mild
Cognitive regression	–	–	–	–
Seizures	–	–	–	–
Initial motor development	normal	normal	normal	normal
Age of onset (years)	3	3	2	4
Motor deterioration	–	–	–	+
Wheelchair use	–	–	–	+
Optic atrophy	–	–	–	–
Myopia	+	+	–	+
Nystagmus	+	+	–	–
Abnormal pursuit	+	+	+	–
Vertical gaze limitation	+	+	+	–
Dysphagia	–	–	+	–
Hypersalivation	–	–	–	–
Cerebellar signs	+	+	+	+
Tremor	–	+	+	+
Babinski refex	–	–	–	–
Spasticity	–	–	mild	–
Peripheral nerve involvement	–	–	–	–
Nerve biopsy	NA	NA	NA	NA
Hypodontia	–	–	–	–
Hypogonadism	+	+	–	–

NA is an abbreviation for not available.

detected with NextGENe. Called SNVs were annotated with SeattleSeq Annotation.

We adopted a prioritization scheme to identify the pathogenic mutation in each individual, similar to the approach taken by recent studies (Table S2).[8–10] First, we excluded the variants registered in the dbSNP131 or 1000 Genome Project from all the detected variants. Then, SNVs commonly detected by MAQ and NextGENe analyses were selected as highly confident variants; 364 to 374 SNVs of nonsynonymous (NS) or canonical splice-site (SP) changes, along with 113 to 124 small insertions or deletions (indels), were identified per individual. We also excluded variants found in our 55 in-house exomes, which are derived from 12 healthy individuals and 43 individuals with unrelated diseases, reducing the number of candidate variants to ~250 per individual. Assuming that HCAHC is an autosomal-recessive disorder based on two affected individuals in one pedigree (individuals 1 and 2), we focused on rare heterozygous variants that are not registered in the dbSNP or in our in-house 55 exomes.

We surveyed all genes in each individual for two or more NS, SP, or indel variants. We found three to eight candidate genes per individual (Table S2). Among them, only *POLR3B* encoding RPC2, the second largest subunit of RNA Polymerase III (Pol III), was common in two individuals (individuals 1 and 3). The inheritance of the variants in *POLR3B* (transcript variant 1, NM_018082.5) was examined by Sanger sequencing. In individual 1, we confirmed that a canonical splice-site mutation (c.1857-2A>C [p.Asn620_Lys652del]), 2 bp upstream of exon 18, was

inherited from his father, and that a missense mutation (c.2303G>A [p.Arg768His]) in exon 21 were inherited from his mother (Figure 1A). The two mutations were also present in an affected elder sister (individual 2) but not present in a healthy elder brother. In individual 3, we confirmed that a nonsense mutation (c.1648C>T [p.Arg550X]) in exon 16 was inherited from her father and that a missense mutation (c.2778C>G [p.Asp926Glu]) in exon 24 was inherited from her mother (Figure 1A). The two mutations were not present in a healthy younger brother. To examine the mutational effects of c.1857-2A>C and c.1648C>T, reverse transcription PCR and sequencing with total RNA extracted from lymphoblastoid cells derived from the individuals was performed as previously described.[11] We demonstrated that the c.1857-2A>C mutation caused deletion of exon 18 from the *POLR3B* mRNA (Figures 2A–2C), resulting in an in-frame 33 amino acid deletion (p.Asn620_Lys652del) from RPC2 (Figure 1B). In addition, the mutated transcript harboring the nonsense mutation (c.1648C>T) was found to be expressed at a much lower level compared with the wild-type transcript (Figure 2D). The expression level of the mutated transcript was increased after treatment with 30 μM cycloheximide (CHX),[11] which inhibits nonsense-mediated mRNA decay (NMD), indicating that the mutant transcript underwent NMD (Figure 2D). The two missense mutations (p.Arg768His and p.Asp926Glu) found in the three individuals occurred at evolutionary conserved amino acids (Figure 1B). Among the other candidate genes in individuals 1 and 3, *MSLN* (MIM 601051), encoding mesothelin isoform 1 preproprotein that is cleaved into megakaryocyte potentiating factor and mesothelin, is a potential candidate in the family of individual 1 as its homozygous variant segregated with the phenotype; however, it is expressed in epithelial mesotheliomas, and the mutation affects less conserved amino acid (Table S3). The other candidate genes' variants did not cosegregate with the phenotype. Thus, mutations in *POLR3B* are most likely to cause HCAHC in two families.

In individual 4, in whom no *POLR3B* mutations were found, there were six candidate genes for an autosomal-recessive model. Among them, *POLR3A* (MIM 614258, GenBank accession number NM_007055.3), harboring two missense mutations, appeared to be a primary candidate because it encodes the largest subunit of Pol III (RPC1) (Figure 1A and Table S2). By Sanger sequencing, we confirmed that a missense mutation (c.2690T>A [p.Ile897Asn]) in exon 20 was inherited from his father and that another missense mutation (c.3013C>T [p.Arg1005Cys]) in exon 23 was inherited from his mother (Figure 1A). The two mutations were not present in a healthy younger sister. The two missense mutations (p.Ile897Asn and p.Arg1005Cys) occurred at relatively conserved amino acids (Figure 1B). In total, we found four mutations in *POLR3B* and two mutations in *POLR3A*. Evaluation of the missense mutations by PolyPhen-2 program showed that three mutations (p.Arg768His,

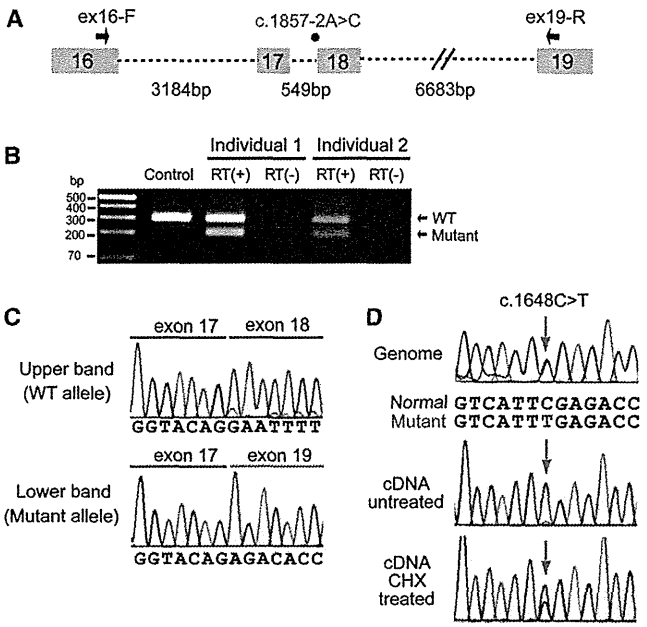

Figure 2. Effects of Splice-Site and Nonsense Mutations in *POLR3B*

(A) Schematic representation of the genomic structure of *POLR3B* from exon 16 to 19. Exons, introns, and primers are shown by boxes, dashed lines, and arrows, respectively. The mutation in intron 17 is depicted as a red dot.

(B) RT-PCR analysis of individuals 1 and 2 with c.1857-2A>C and a normal control. Two PCR products were detected from the individual's cDNA: the upper band is the wild-type (WT) transcript, and the lower band is the mutant. Only a single wild-type amplicon was detected in the control.

(C) Sequence of WT and mutant amplicons clearly showed exon 18 skipping in the mutant allele.

(D) Analysis of the c.1648C>T mutation. Sequence of PCR products amplified with genomic (upper), cDNA from untreated cells (middle), and cDNA from CHX treated cells (lower) as a template. Although untreated cells show extremely low levels of c.1648C>T mutant allele expression, cells treated to inhibit NMD show significantly increased levels of mutant allele expression.

p.Asp926Glu, and p.Ile897Asn) were probably damaging and that p.Arg1005Cys is tolerable. The c.2303G>A mutation (*POLR3B*) was found in one allele out of 540 Japanese control chromosomes. The remaining five mutations were not detected in 540 Japanese control chromosomes, indicating that the mutations are very rare in the Japanese population. Among the other candidate genes in individuals 4, *IGSF10*, a member of immunoglobulin superfamily, is a potential candidate because its variants segregated with the phenotype (Table S3); however, considering a close relationship between *POLR3A* and *POLR3B*, and the fact that *POLR3A* mutations have been recently reported in hypomyelinating leukodystrophy (see below),[12] *POLR3A* abnormality is the most plausible culprit for HCAHC in individual 4.

The structure of Pol III[13,14] and Pol II[15,16] is highly homologous, especially in the largest subunits. Thus, we extrapolated the mutations of RPC1 or RPC2 onto the structure of yeast Pol II (Protein Data Bank [PDB] accession number 3GTP)[17] (Figure 1C). RPB1 and RPB2 subunits of